A&A 477, 293–298 (2008)
DOI: 10.1051/0004-6361:20078208

Astronomy & Astrophysics

Characteristics of plasma turbulence and radio emission from an interplanetary shock wave

V. G. Ledenev[1], E. Aguilar-Rodriguez[2], V. V. Tirsky[3], and V. M. Tomozov[1]

[1] Institute of Solar-Terrestrial Physics, Russian Academy of Sciences, PO Box 291, Irkutsk, Russia
e-mail: leden@iszf.irk.ru
[2] Space Sciences Laboratory, University of California, Berkeley, USA
[3] Institute of Laser Physics, Russian Academy of Sciences, Irkutsk Branch, Russia

Received 3 July 2007 / Accepted 6 October 2007

ABSTRACT

Aims. We investigate the characteristics of energetic electron beams, plasma turbulence and radio emission from interplanetary shock waves.
Methods. Numerical calculations of spectra and Landau damping of hot plasma eigen oscillations in the magnetic field are used.
Results. It is shown that the longitudinal wave spectrum, excited in the solar wind plasma, extends with the increase of the refractive index n over range of values $n > 10$. This result allows us to explain the broad band of emission, the constant value of the average ratio of frequency-band to radio emission frequency from interplanetary shock wave fronts, and to estimate the electron beam density and amplitude of Langmuir waves at the shock. It is shown that a spectrum of radio emission is determined by the spectrum of Langmuir waves excited upstream of the interplanetary shock wave by heated electrons escaping from the shock wave front.

Key words. Sun: solar wind – Sun: radio radiation – shock waves

1. Introduction

At the present time, much observational data has been accumulated concerning the structure of interplanetary shock waves (ISW), their connection with coronal mass ejections and their radio emission, which is generated at ISW fronts and covers a wide range of wavelengths, from decameter to kilometric domains (Cane et al. 1981, 1982, 1987; Lengyel-Frey & Stone 1989; Reiner et al. 1998; Gopalswamy et al. 2001). However, the first observations from spacecraft (ISEE-3 and WIND) did not answer the question of whether radio emission is generated upstream or downstream of the ISW (Lengyel-Frey 1992). Bale et al. (1999) performed the first direct observation of the source region of a type II radio burst upstream of ISW. In models of radio emission generation at ISW fronts, it is assumed that the emission is generated due to transformation of the longitudinal plasma waves which are excited by energetic electron beams accelerated at the ISW front (Bale et al. 1999; Knock et al. 2001, 2003; Cairns et al. 2003). In these models electrons were accelerated through reflection from the magnetic mirror in the front of the shock. Models based on the assumption that longitudinal waves are generated by the part of an adiabatically heated electron population that escapes from the ISW front was suggested by Ledenev (1996). Smith (1971) had proposed earlier an analogous model for the interpretation of type II solar radio emission bursts in the meter wave range. The formation of electron beams upstream of the Earth's bow shock was investigated by Filbert & Kellogg (1979), Wu (1984), Leroy & Mangeney (1984). In this paper we suppose as in Ledenev (1996) that longitudinal waves are generated by the electron population, which escapes from the ISW front, but that electron heating and acceleration occurs through instabilities developed in the shock. The energetic electron flux upstream of the strong shock is determined by interaction with plasma turbulence developed through these instabilities. This means that temperatures of electrons and ions behind a density jump at the shock in a general way are different from adiabatic values. In our opinion, electron acceleration through reflection from the magnetic mirror is not effective under conditions of developed plasma turbulence.

One of the intriguing characteristics of ISW radio emission is a broad band of emission which can reach up to 40% of the central frequency in some events. Moreover, the mean ratio of the frequency-band to the central emission frequency is approximately constant, with a value of 0.25−0.3 for the several hundred events that were analyzed by Aguilar-Rodriguez et al. (2005) in the decametric-hectometric and kilometric wavelength domains. Metric type II bursts are also broadband events and the mean ratio of the frequency-band to the low instantaneous emission frequency is 0.32 and 0.37 for fundamental and harmonic emission bands, respectively (Mann et al. 1995). Such a wide frequency band that is observed at metric, decametric-hectometric, and kilometric wavelength domains is explained by density and plasma frequency jumps at weak shocks with a ratio of downstream and upstream densities of less than 2.5 (Mann et al. 1995; Vršnak et al. 2002). At the same time, the density jump at stronger shocks may reach a value of 4 (Tidman & Krall 1971). To interpret these observational data we use such properties of plasma waves as broadening of the frequency band in the region of refractive index $n > 10$, which allows us to estimate density and energy of the electron beam at the front of the ISW and avoid restriction of the shock wave intensity.

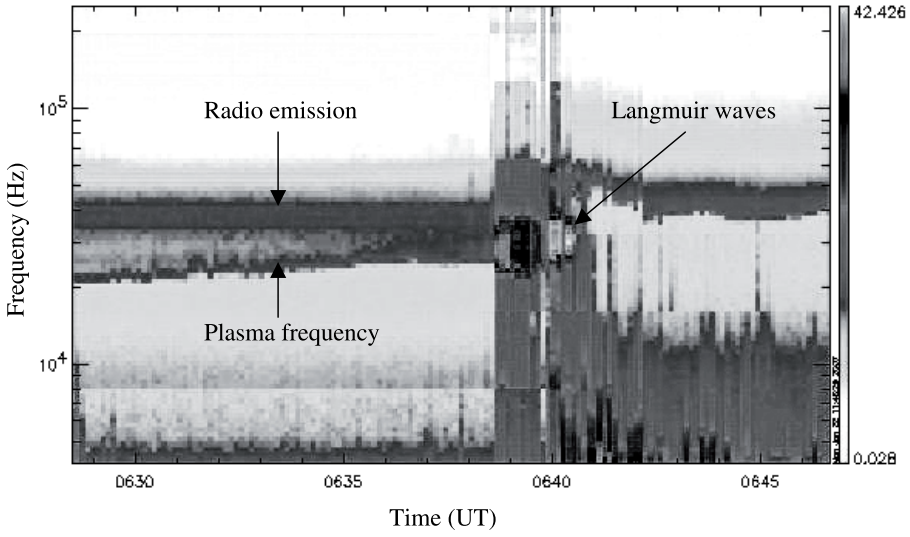

Fig. 1. Spectrogram during the passage of an interplanetary shock wave, observed by the Thermal Noise Receiver (TNR) instrument of Wind/WAVES on 26 August 1998.

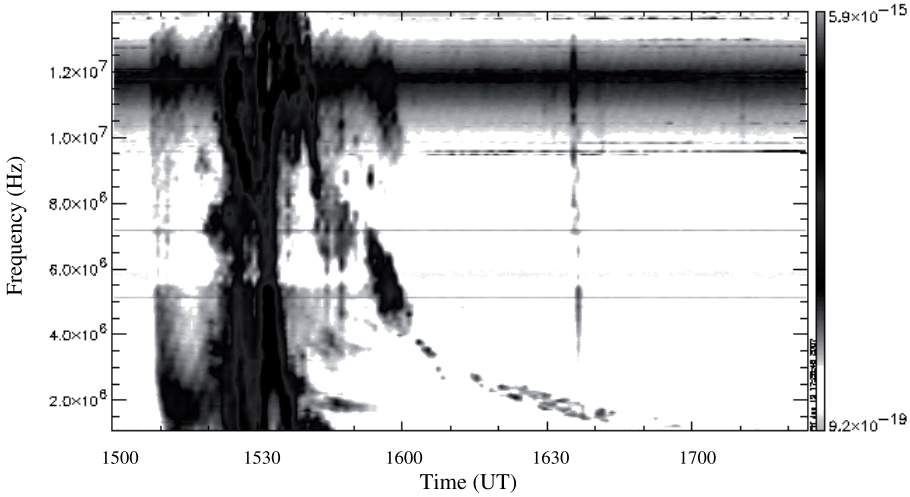

Fig. 2. Spectrogram of a type II radio burst, in the decametric-hectometric wavelength range, observed by the WAVES/RAD2 receiver on 6 June 2000.

2. Observations

The Radio and Plasma Waves Experiment (WAVES) (Bougeret et al. 1995) on board the Wind spacecraft has three receivers (TNR, RAD1, and RAD2), which record radio emission over a wide range of frequencies (4−256 kHz, 20−1040 kHz, and 1.075−13.825 MHz). Figure 1 shows the spectrogram of the well-studied Wind/WAVES passage through a strong (Mach number M ≈ 10) quasi-perpendicular ISW (Bale et al. 1999) on 26 August 1998 in the kilometer wavelength domain. Some of the most interesting observational features of this event are (1) the frequency of the radio emission is higher than the plasma frequency at the maximum of the Langmuir wave intensity, (2) the upper and the lower boundaries of the radio emission are very steady, and (3) the frequency band of the radio emission is wide (∼30%) and almost constant. Figure 2 shows the spectrogram of a type II burst, in the decametric-hectometric wavelength range, observed by Wind/WAVES on 6 June 2000. The type II burst is reported on the Wind/WAVES list, maintained by M. L. Kaiser (`http://www-lep.gsfc.nasa.gov/waves/waves.html`), as an intense and complex fundamental emission with an intermittent harmonic. By considering the fundamental band of emission, we notice that there are three bright regions: (1) the first at ∼15:40 UT at ∼12 MHz, (2) the second at ∼15:58 UT at ∼6 MHz, and (3) the third at ∼16:30 UT at ∼2 MHz. The ratio of the frequency band to the central emission frequency is almost constant for these bright regions, and is calculated to be around ∼30%.

3. High-frequency waves in interplanetary plasma

Spectra of eigen oscillations in solar wind plasmas are determined on the basis of the numerical solution of the dispersion relation for hot magnetized plasma. This relation was solved for conditions of the Earth's magnetosphere by Andre (1985). The solution for the solar corona was obtained by Ledenev et al. (2006), and Ledenev & Tirsky (2006). These computations show that characteristics of longitudinal waves in hot magnetized plasma may be different to those of cold plasma.

The spectra of high-frequency eigen oscillations of interplanetary plasma are coincident with spectra of isotropic plasma oscillations because the interplanetary magnetic field is so weak that it does not influence the oscillations. The interplanetary magnetic field is much weaker than the solar corona magnetic field. The weak effect of the magnetic field on the interplanetary plasma is demonstrated by comparing the ratio of electron cyclotron frequency to electron plasma frequency (in the interplanetary plasma, $\omega_{He}/\omega_{pe} \sim 10^{-2}$, and in solar corona $\omega_{He}/\omega_{pe} \sim 10^{-1}$). Nevertheless, the influence of the magnetic field is essential for the formation of energetic electron beams escaping

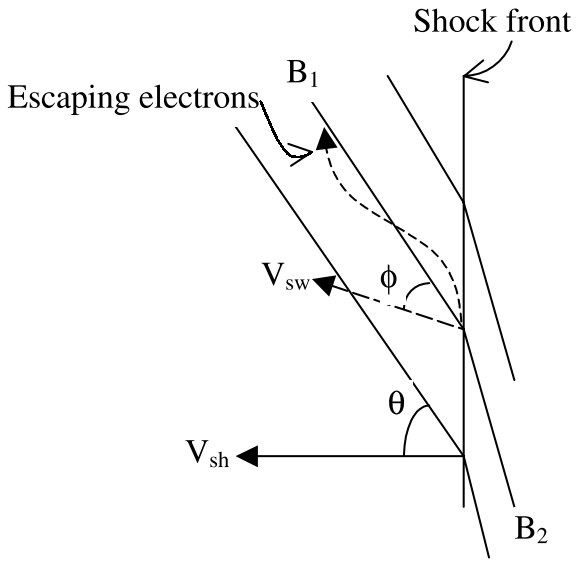

Fig. 3. A schematic representation of a shock geometry that shows that the influence of the magnetic field is essential for the formation of energetic electron beams escaping from the shock wave front, because these electrons are moving along the magnetic field. B_1 and B_2 are the magnetic fields ahead and behind of the shock wave front, V_{sh} is the shock velocity in the direction of the normal to the shock front, V_{sw} is the solar wind velocity.

from the shock wave front (Ledenev 1996), because these electrons are moving along the magnetic field (see Fig. 3). At the same time, spectra of longitudinal waves in hot interplanetary plasma are different to those in cold plasma due to the dependence of the wave frequency on the plasma temperature and the wavelength. The plasma temperature determines the maximum values of the refractive index (minimum phase velocities) of weakly damping longitudinal waves. The frequency of longitudinal waves grows when the refractive index approaches these values (Ledenev et al. 2006; Ledenev & Tirsky 2006). Weakly damping waves are the ones whose damping rate is not higher than 0.1 ω (ω is the frequency of waves excited by electron beam upstream of the shock front).

To determine the eigen oscillation spectra in the interplanetary plasma, we solved numerically the equation that describes dispersion characteristics of hot magnetized plasma (Akhiezer et al. 1975; Ginzburg & Rukhadze 1975):

$$\left\{a + \left(\frac{\omega}{kc}\right)^2 b + \left(\frac{\omega}{kc}\right)^4 c_0\right\} = 0, \tag{1}$$

where

$$a = \left(\frac{k_\perp}{k}\right)^2 \epsilon_{xx} + \left(\frac{k_z}{k}\right)^2 \epsilon_{zz} + 2\left(\frac{k_\perp k_z}{k^2}\right)\epsilon_{xz},$$

$$b = -\epsilon_{xx}\epsilon_{zz} + \epsilon_{xz}^2 - \left(\frac{k_z}{k}\right)^2 \left(\epsilon_{yy}\epsilon_{zz} + \epsilon_{yz}^2\right) - \left(\frac{k_\perp}{k}\right)^2 \left(\epsilon_{xx}\epsilon_{yy} + \epsilon_{xy}\right)^2 + 2\left(\frac{k_\perp k_z}{k^2}\right)\left(\epsilon_{xy}\epsilon_{yz} - \epsilon_{xz}\epsilon_{yy}\right),$$

$$c_0 = \epsilon_{zz}\left(\epsilon_{xx}\epsilon_{yy} + \epsilon_{xy}\right)^2 + \epsilon_{xx}\epsilon_{yz}^2 - \epsilon_{yy}\epsilon_{xz}^2 + 2\epsilon_{yz}\epsilon_{xz}\epsilon_{xy},$$

$$\epsilon_{xx} = 1 - \sum_s \frac{s^2\omega_{pe}^2}{\omega(\omega - s\omega_{He})}\frac{A_s(Z)}{Z}J(\beta_s),$$

$$\epsilon_{yy} = \epsilon_{xx} + 2\sum_s \frac{\omega_{pe}^2 Z}{\omega(\omega - s\omega_{He})}A_s'(Z)J(\beta_s),$$

$$\epsilon_{xy} = -\epsilon_{yx} = -i\sum_s \frac{s\omega_{pe}^2}{\omega(\omega - s\omega_{He})}A_s'(Z)J(\beta_s),$$

$$\epsilon_{xz} = \epsilon_{zx} = \sum_s \frac{s\omega_{pe}^2 k_\perp}{\omega\omega_{He}k_z}\frac{A_s(Z)}{Z}\left[1 - J(\beta_s)\right],$$

$$\epsilon_{yz} = -\epsilon_{zy} = -i\sum_s \frac{\omega_{pe}^2 k_\perp}{\omega\omega_{He}k_z}A_s'(Z)\left[1 - J(\beta_s)\right],$$

$$\epsilon_{zz} = 1 + \sum_s \frac{\omega_{pe}^2(\omega - s\omega_{He})}{\omega k_z^2 v_{Te}^2}A_s(Z)\left[1 - J(\beta_s)\right].$$

Here ω is the complex wave frequency, c the speed of light in a vacuum, k_z the longitudinal (with respect to the magnetic field) wave vector component, $k_\perp$ the transverse wave vector component, and ϵ_{ij} stands for the components of the dielectric tensor, $A_s(Z) = \exp(-Z)I_s(Z)$, $I_s(Z)$ is a modified Bessel function, $Z = k_\perp^2 v_{Te}^2/\omega_{He}^2$, $\beta_s = (\omega - \omega_{He})/k_z v_{Te}$, $J(Z) = -i\sqrt{\frac{\pi}{2}}ZW(\frac{Z}{\sqrt{2}})$, $W(x)$ is the probability integral, s the number of the cyclotron harmonic. The formulae transformed for numerical calculations are given by Ledenev et al. (2006) and Ledenev & Tirsky (2006).

The dielectric tensor components were calculated by summation over cyclotron harmonics. The weaker the magnetic field, the more harmonics must be included to provide the required computational precision, and it is necessary to provide the summation up to the maximal number of cyclotron harmonic $s_{max} \sim k_\perp v_\perp/\omega_{He}$ (Ginzburg & Rukhadze 1975). The maximal value of the wave number of longitudinal waves that can generate kilometric radiation is $k_{max} \sim \omega/v_{Te} \sim 10^{-3}$ cm^{-1}, where $\omega \sim 10^5$ s^{-1} is the radiation frequency, and $v_{Te} \sim 10^8$ cm s^{-1} is the thermal velocity of electrons. Accordingly, the maximal number of cyclotron harmonics in the case $k_z \gg k_\perp$ is $s_{max} \sim 0.1 k_{max} v_{Te}/\omega_{He} \sim 10$, for the magnetic field of ~10 nT (for the cyclotron frequency $\omega_{He} \sim 10^3$ s^{-1}). In these calculations, we performed the summation up to the fifteenth harmonic.

Electrons escaping from the shock wave front move along the magnetic field, and wave vectors of plasma waves excited by these electrons are directed mainly along the magnetic field. Therefore calculations of dispersion characteristics are made for waves propagating almost along the magnetic field. The frequency dependence of the refractive index $n = kc/\omega$ for weak-damped (damping rate $\gamma < 0.1\ \omega$) eigen oscillations in the interplanetary plasma, for wave propagation at small angles to the magnetic field, is given in Fig. 4. At other angles the dispersion dependencies are almost the same because the solar wind plasma is practically isotropic. Therefore we assume that in this case the behavior of the dispersion curves is invariable in a broad angle range up to about 90°. Calculations were made for the following values of the plasma parameters: $\omega_{He}/\omega_{pe} = 10^{-2}$, $v_{Te}/c = 0.5 \times 10^{-2}$, $\theta_0 = 0.1$ radian (θ_0 is the angle between the wave vector and the magnetic field). As seen from Fig. 4, dispersion curves of transverse electromagnetic waves (branches 1, 2, which correspond to extraordinary and ordinary modes) are practically merged, and their behavior is similar to electromagnetic waves in cold plasma. However, the characteristics of the longitudinal waves (branch 3) for a refractive index larger than 10 differ substantially from longitudinal wave characteristics in cold plasma, namely, with increased refractive index the longitudinal wave frequency increases. This increase is limited by the growth of Landau damping when the phase velocity of waves

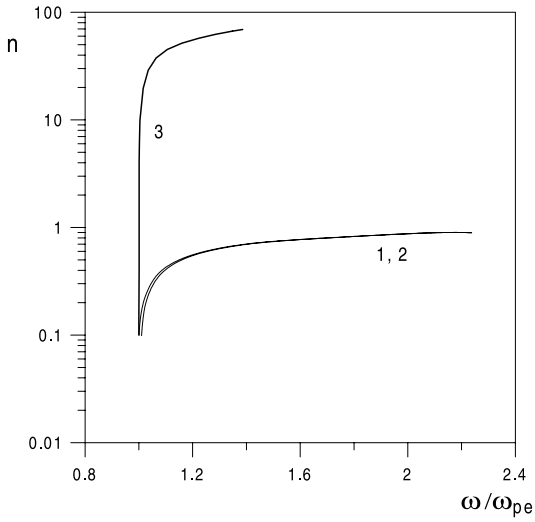

Fig. 4. Frequency dependence of refractive index for $\omega_{pe}/\omega_{He} = 100$, $v_{Te}/c = 0.5 \times 10^{-2}$, $\theta_0 = 0.1$ radian. Branches 1 and 2 are plots for extraordinary and ordinary waves respectively. Branch 3 corresponds to longitudinal waves.

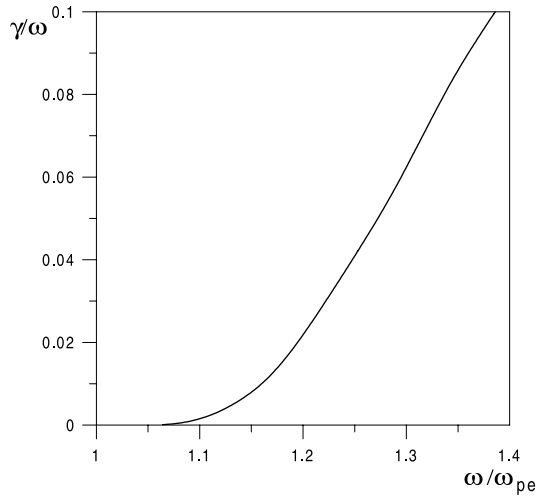

Fig. 5. Frequency dependence of Landau damping for plasma parameters corresponding to Fig. 4.

approaches the electron thermal velocity. At values of the wave frequency close to 1.4 ω_{pe} the damping achieves a value ~0.1 ω. This means that in a homogeneous plasma, longitudinal waves can be excited in the frequency band up to ~0.4 ω_{pe}.

Landau damping dependence on frequency for the above-mentioned parameters is shown in Fig. 5. In a weak magnetic field ($\omega_{He}/\omega_{pe} \ll 1$) this dependence is practically unchanged with changes in the plasma temperature and the angle between the wave vector and the magnetic field, since, as is shown by calculations (Ledenev et al. 2006), the dispersion characteristics of longitudinal waves depend weakly on the angle θ_0. The plasma temperature affects the maximally achievable values of the refractive index (the phase velocities of low-damping waves decrease with temperature increasing and vice-versa) and does not change the shape of the dispersion curves.

4. Discussion and interpretation of observational data

High-frequency plasma turbulence at the ISW front may be excited by electrons accelerated by the shock wave front up to energies much greater than the thermal electron energy (Cairns et al. 2003; Mann & Klassen 2005). The electron energy corresponds to high phase velocities of longitudinal waves excited by these electrons. As seen from Fig. 4, such waves are excited in a narrow band of frequency. But the observational data show (Bale et al. 1999; Aguilar-Rodriguez et al. 2005) that in most cases spectra of longitudinal waves and radio emission occupied a broad frequency band, and radio emission frequency band is situated in the region higher than frequency of the most intensive plasma waves (Langmuir waves, see Fig. 1). Most intensive Langmuir waves are excited at frequencies close to the local plasma frequency, but electromagnetic waves at such frequencies are damped. Only electromagnetic waves with frequencies higher than the plasma frequency can be emitted. This means that radio emission is generated by the longitudinal wave spectrum which covers the phase velocity range up to values close to (3−5) v_{Te}. Therefore it is more natural, in our opinion, to assume that this turbulence may be excited by heated electrons leaving the ISW front (Ledenev 1996). The maximum density of outgoing electrons corresponds to their minimal velocity. Therefore plasma waves with low phase velocities can be excited upstream of the shock wave front, and their frequency may be significantly higher than the local plasma frequency.

The minimum velocity for electrons leaving the shock is equal to the velocity of the ISW. These electrons do not excite plasma turbulence, because ISW velocity, in most cases, is lower than the thermal velocity of the electrons. If the ISW propagates at a certain angle to the magnetic field, the velocity of electrons leaving the shock front will be higher at larger angles between the shock front normal and the magnetic field (see Fig. 3) (Ledenev 1996). The electrons that escape the shock must have a velocity along the field $V \sim V_{sh}/\cos\theta$. Here θ is the angle between the normal to the shock front and the magnetic field. If $V > 3v_{Te} + V_{sw}\cos\phi$, plasma waves are excited ahead of the shock front. Here v_{Te} is the electron thermal velocity upstream of the shock front, V_{sw} the solar wind velocity, and ϕ the angle between the velocity vector of the solar wind and the magnetic field. Typical shock velocities in the solar wind are 10^7–10^8 cm s^{-1}. The thermal velocity of electrons is $v_{Te} \sim 10^8$ cm s^{-1} for a temperature $T \sim 10^5$ K. For strong enough shock waves and low solar wind velocity the velocity of electron beams that drive plasma waves must be larger than $3v_{Te}$ (~3×10^8 cm s^{-1}). Accordingly, the angle θ for shocks that generate the emission must be $\theta > 70°$.

Observations show that the mean ratio of the radio emission band to the central frequency upstream of the ISW front is ~25–30% (Farrell et al. 2004; Aguilar-Rodriguez et al. 2005). One of the observations is presented in Fig. 2. As our calculations show, the frequency band of plasma waves excited by electrons escaping from the shock front may be about 0.4 ω_{pe}. The corresponding central frequency is ~1.2 ω_{pe}. Then the frequency band of plasma waves is ~30% of the plasma wave central frequency. The obtained estimation of the emission frequency band shows a good agreement with observations. In the event on 26 August 1998 (see Fig. 1), the upper boundary of the emission band (~40 kHz) is about 30% higher than upper frequency of the most intensive Langmuir turbulence (~30 kHz). The corresponding emission frequency band is ~30% of the central frequency. This means that the radio emission spectrum is determined by the Langmuir wave spectrum. Landau damping of longitudinal waves excited by the electron beam causes the sharp upper boundary of the emission band. The lower boundary is caused by

emission damping near the plasma frequency at the shock front. As seen from Fig. 4, such a frequency of the longitudinal waves ($\sim 1.3\ \omega_{pe}$) corresponds to the refractive index value $n \sim 60$. This means that the phase velocity of longitudinal waves, and, consequently, the velocity of energetic electrons, is about three times greater than the thermal electron velocity of plasma, for which the dispersion curves were calculated (see Fig. 4). If the thermal electron energy upstream of the ISW front is ~10 eV, the energy of electrons, which pass ahead of the ISW front and excite longitudinal waves is, ~100 eV. This well agrees with observations of electron energies upstream of the ISW front (Bale et al. 1999) which show that the energy is in the range 100−150 eV.

The main damping mechanism in the solar wind is Landau damping on thermal electrons. According to the plot in Fig. 5, the band of longitudinal waves of ~30% corresponds to the damping rate $\gamma \approx 0.06\ \omega$. The linear growth rate of longitudinal waves must be not less than this value. The growth rate for the beam instability in isotropic plasma is $\gamma_b \sim (n_b/n_0)\omega_{pe}$ (Mikhailovsky 1974). Here n_b is the electron beam density, n_0 is the plasma density before the shock front. Hence, we estimate the electron flux density at the ISW front $n_b/n_0 \sim 0.1$.

The plasma heating at the shock front takes place due to development of low-frequency instabilities which play the role of effective viscosity. Papadopoulos (1988) proposed an electron energization process in high Mach number shocks, in which electron heating is produced through two-step instabilities in the shock front where the reflected ions coexist with the incident ions and electrons. Buneman instability (BI) is first excited by the velocity difference between the reflected ions and the incident electrons, and the electrons are heated up by the instability. The ion acoustic instability then is triggered under the pre-heated electron plasma by BI, and the electrons are further heated up. At the same time, temperatures of electrons and ions in the region of instability development are in the general case different from one another and from the value obtained from general relations at a shock front. Numerical calculations (Shimada & Hoshino 2000) show that electrons behind a shock front not only are heated, but they are also accelerated with creation of the nonthermal tail. The density of nonthermal electrons may be about 10% of the density in the shock front in strong shock waves with an Alfven Mach number $M \sim 10$. Some of these electrons, with the velocity $V > V_{sh}/\cos\theta$, move along the magnetic field and pass ahead of the shock wave with formation of an unstable distribution function. The density of these electrons may be about 10% of the plasma density upstream of the shock front even with taking into account that velocities of these electrons are directed mainly along the magnetic field. These electrons excite intense plasma turbulence ahead of the density jump in the shock wave front. Thus our estimation of the energetic electron density upstream of the shock is not contrary to the numerical calculation by Shimada & Hoshino (2000).

The energy density of plasma waves excited by an electron beam may be evaluated considering the boundary problem of an electron beam injection into a half-space filled with plasma (Vedenov & Ryutov 1975). In this case the energy density of plasma waves is $W^l \approx m n_b v_b^4/15 v_{Te}^2$, where v_b is the electron beam velocity ahead of the shock front. For higher estimations of density and energy of electrons leaving the shock front we have $W^l \sim 10^{-11}$ erg cm^{-3}. The corresponding amplitude of the plasma wave electric field is $E \sim 10^{-6}$ statvolt cm^{-1} or in the SI system, $E \sim 30$ mV m^{-1}. This value agrees well with direct measurements during the event shown in Fig. 1, which gives $E \sim 40$ mV m^{-1}.

The velocity of electrons escaping from the ISW front depends on many factors, including the shock wave intensity, the angle between the direction of the ISW propagation and the magnetic field. The more energetic electrons excite waves with higher phase velocities, i.e. as seen from Fig. 4, they generate waves in a narrow band of frequencies. This case corresponds to a small ratio of the emission band to the frequency, and is observed for some shocks (Aguilar-Rodriguez et al. 2005).

At the same time, the shock front is not a planar structure. Observations (Bale et al. 1999) suggest evidence of large-scale structure on the shock front. This means that the bandwidth of Langmuir waves on the shock front is broad (Fig. 1), and thus the radio emission bandwidth may enlarge and reach a value of 0.7−0.8 (Aguilar-Rodriguez et al. 2005). Lengyel-Frey & Stone (1989) and Aguilar-Rodriguez et al. (2005) showed that the emission bandwidth from the ISW front decreases with increasing the heliocentric distance. This can be explained as the ISW weakening with propagation, causing a decrease of the large-scale structure effect in the ISW front.

We assume that the radio emission is mainly generated close to the plasma wave frequency by scattering of the waves by ion-acoustic turbulence, which is excited in the ISW front by reflected ions (Melrose 1980; Ledenev 1996). This means that the most intensive radio emission is generated in the shock front, and its frequency band is determined by the plasma wave band.

5. Conclusions

Observations of radio emission from ISW fronts, obtained by the ISEE-3 and WIND spacecraft, show that the average ratio of the radiation band to the central frequency of radiation is roughly constant and is equal to 25−30% (Farrell et al. 2004; Aguilar-Rodriguez et al. 2005). The interpretation of these observational data is difficult in the framework of present concepts about generation of the radio emission by electrons accelerated on the ISW front (Cairns et al. 2003; Mann & Klassen 2005). The main reason is that the electrons are accelerated up to energies that greatly exceed the thermal electron energy before the ISW front. This means that the longitudinal waves that are generated by fluxes of energetic electrons and afterwards transformed into radio emission must be excited in a narrow band of frequencies close to the local plasma frequency. This discrepancy can be overcome if we assume that the radio emission is generated by part of a heated and partly accelerated electron population escaping from the ISW front. These electrons have a broad spectrum of energies with a maximum lying in the lower energy range corresponding to electrons leaving the ISW front. Their energies exceed by an order of magnitude the thermal electron energy before the ISW front.

Our calculations of the dispersion characteristics of eigen oscillations in the plasma with a weak magnetic field show that in the conditions of the solar wind plasma, the frequency of longitudinal waves increases when the refractive index grows in the range of values $n > 10$, i.e. when the wave phase velocity approaches the thermal velocity of the electrons. These results allow us to explain the existence of broadband emission from the ISW front and the average constancy of the ratio of the frequency band to the central emission frequency, and to derive estimates of electron flux parameters and the plasma wave electric field.

Acknowledgements. We are indebted to M. Pulupa for useful comments on the manuscript. We also wish to thank ind/WAVES team, and in particular M. L. Kaiser, for the use of their online data. E. Aguilar-Rodriguez thanks the UC MEXUS CONACyT program. The authors thank the referee for the comments that have improved this manuscript.

References

Aguilar-Rodriguez, E., Gopalswamy, N., MacDowall, R., Yashiro, S., & Kaiser, M. L. 2005, JGR, 110, A12S08

Akhiezer, A. I., Akhiezer, I. A., Polovin, R. V., Sitenko, A. G., & Stepanov, K. N. 1975, Plasma Electrodynamics (Oxford: Pergamon Press)

Andre, M. 1985, J. Plasma Phys., 33, 1

Bale, S. D., Reiner, M. J., Bougeret, J. L., et al. 1999, GRL, 26, 1573

Bougeret, J. L., Kaiser, M. L., Kellogg, P. J., et al. 1995, Space Sci. Rev., 71, 231

Cairns, I. H., Knock, S. A., Robinson, P. A., & Kuncic, Z. 2003, Space Sci. Rev., 107, 27

Cane, H. V., Stone, R. G., Fainberg, J., et al. 1981, GRL, 12, 1285

Cane, H. V., Stone, R. G., Fainberg, J., Steinberg, J.-L., & Hoang, S. 1982, Sol. Phys., 78, 187

Cane, H. V., Sheeley, N. R., & Howard, R. A. 1987, JGR, 92, 9869

Farrell, W. M., Kaiser, M. L., Bale, S. D., et al. 2004, JGR, 109, A02106

Filbert, P. C., & Kellogg, P. J. 1979, JGR, 84, 1369

Ginzburg, V. L., & Rukhadze, A. A. 1975, Waves in Magnetoactive Plasma (M. Nauka)

Gopalswamy, N., Yashiro, S., Kaiser, M. L., Howard, R. A., & Bougeret, J. L. 2001, JGR, 106, 29219

Knock, S. A., Cairns, I. H., Robinson, P. A., & Kuncic, Z. 2001, JGR, 106, 25041

Knock, S. A., Cairns, I. H., Robinson, P. A., & Kuncic, Z. 2003, JGR, 108, 1126

Ledenev, V. G. 1996, A&A, 316, 435

Ledenev, V. G., & Tirsky, V. V. 2006, Radiophys. Quantum Electron., 49, 231

Ledenev, V. G., Tirsky, V. V., & Tomozov, V. M. 2006, A&A, 452, 339

Lengyel-Frey, D. 1992, JGR, 97, 1609

Lengyel-Frey, D., & Stone, R. G. 1989, JGR, 94, 159

Leroy, M. M., & Mangeney, A. 1984, Ann. Geophys., 2, 449

Mann, G., & Klassen, A. 2005, A&A, 441, 319

Mann, G., Classen, T., & Aurass, H. 1995, A&A, 295, 775

Melrose, D. B. 1980, Plasma Astrophysics (New York: Gordon and Breach)

Mikhailovsky, A. B. 1974, Theory of Plasma Instabilities (New York: Consultant Bureau)

Papadopoulos, K. 1988, Astrophys. Space Sci., 144, 535

Reiner, M. J., Kaiser, M. L., Fainberg, J., & Stone, R. G. 1998, JGR, 103, 29651

Shimada, N., & Hoshino, M. 2000, ApJ, 543, L67

Smith, D. F. 1971, ApJ, 170, 559

Tidman, D. A., & Krall, N. A. 1971, Shock Waves in Collisionless Plasmas (New York: Wiley-Interscience)

Vedenov, A. A., & Ryutov, D. D. 1975, Rev. Plasma Phys., 6, 1

Vršnak, B., Magdalenić, J., Aurass, H., & Mann, G. 2002, A&A, 396, 673

Wu, C. S. 1984, JGR, 89, 8857